



1 **Global patterns of soil organic carbon dynamics in the 20–100 cm soil profile for**  
2 **different ecosystems: A global meta-analysis**

3 Haiyan Wang<sup>1,2</sup>, Yulong Yin<sup>1,\*</sup>, Tingyao Cai<sup>1</sup>, Xingshuai Tian<sup>1</sup>, Zhong Chen<sup>1</sup>, Kai  
4 He<sup>1</sup>, Zihan Wang<sup>1</sup>, Haiqing Gong<sup>1</sup>, Qi Miao<sup>1</sup>, Yingcheng Wang<sup>1</sup>, Yiyan Chu<sup>1</sup>,  
5 Qingsong Zhang<sup>1,2,\*</sup>, Minghao Zhuang<sup>1</sup>, Zhenling Cui<sup>1,\*</sup>

6 <sup>1</sup> State Key Laboratory of Nutrient Use and Management, College of Resources and  
7 Environmental Sciences, China Agricultural University, 100193 Beijing, China

8 <sup>2</sup> Sanya Institute of China Agricultural University, 572025 Sanya, China

9 **\*Corresponding author:** Zhenling Cui. Email: [cuizl@cau.edu.cn](mailto:cuizl@cau.edu.cn)

10 Yulong Yin. Email: [yinyulong88221@163.com](mailto:yinyulong88221@163.com)

11 Qingsong Zhang. Email: [zhangqs@cau.edu.cn](mailto:zhangqs@cau.edu.cn)

12

13 **Manuscript submitted to: Earth System Science Data**



14 **Abstract**

15 Determining the dynamics of organic carbon in subsoil (SOC, depth of 20–100 cm) is  
16 important with respect to the global C cycle and warming mitigation. However, there  
17 is still a huge knowledge gap in the dynamics of spatiotemporal changes in SOC in  
18 this layer. Combining traditional depth functions and machine-learning methods, we  
19 achieved soil  $\beta$  values and SOC dynamics at high resolution for global ecosystems  
20 (cropland, grassland, and forestland). First, quantified the spatial variability  
21 characteristics of soil  $\beta$  values and driving factors by analyzing 1221 soil profiles (0–  
22 100 cm) of globally distributed field observations. Then, based on multiple  
23 environmental variables and soil profile data, we mapped the grid-level soil  $\beta$  values  
24 with machine-learning approaches. Lastly, we evaluated the SOC density spatial  
25 distribution in different soil layers to determine the subsoil SOC stocks of various  
26 ecosystems. The subsoil SOC density values of cropland, grassland, and forestland  
27 were 63.8, 83.3, and 100.4 Mg ha<sup>-1</sup>, respectively. SOC density decreased with  
28 increasing depth, ranging from 5.6 to 30.8 Mg ha<sup>-1</sup> for cropland, 7.5 to 40.0 Mg ha<sup>-1</sup>  
29 for grassland, and 9.6 to 47.0 Mg ha<sup>-1</sup> for forestland. The global subsoil SOC stock  
30 was 912 Pg C (cropland, grassland, and forestland were 67, 200, and 644 Pg C), in  
31 which an average of 54% resided in the top 0–100 cm of the soil profile. This study  
32 provides information on the vertical distribution and spatial patterns of SOC density at  
33 a 10 km resolution for areas of Global ecosystems, which providing a scientific basis  
34 for future studies pertaining to Earth system models. The dataset is open-access and  
35 available at <https://doi.org/10.5281/zenodo.10846543> (Wang et al., 2024).

36 **Keyword:** Subsoil SOC dynamics; Soil profiles; Random forest; Driving factors;  
37 Global ecosystems

38



## 39 **1. Introduction**

40 Organic carbon in soil (SOC) plays a critical role in global C cycling, climate change  
41 mitigation, reducing greenhouse gas(GHG) emissions, and the health of ecosystems  
42 (Bradford et al., 2016; Lal et al., 2021; Griscom et al., 2017) Subsoil, defined here as  
43 soil residing below 20 cm in depth, contains more than half of the global SOC stock  
44 (Esteban G. Jobb gy. and Jackson., 2000; Poffenbarger et al., 2020; Batjes, 1996).  
45 Worldwide, high SOC loss due to crop production and grazing, which contributes  
46 significantly to increasing atmospheric CO<sub>2</sub> levels (Beillouin et al., 2023; Lal, 2020;  
47 Qin et al., 2023). Complex polymeric carbon in subsoil is vulnerable to decomposition  
48 under future warming; specifically, ecological or trophic limitations of SOC  
49 biodegradation in deep soil layers can lead to sharp declines in the nutrient supply and  
50 biodiversity (Chen et al., 2023). Subsoil is more suited to long-term C sequestration  
51 than topsoil. The ‘4 per 1000’ initiative aims to boost SOC storage in agricultural  
52 soils by 0.4% each year to help mitigate climate change and increase food security  
53 (Chabbi et al., 2017). However, subsoil SOC dynamics, especially across a large  
54 scale, remain poorly understood (Padarian et al., 2022), as the measurements are  
55 difficult, time-consuming, and labor intensive particularly at deeper depths.

56 Recent studies have focused on SOC allocation and dynamics at varied depths and the  
57 subsoil SOC–climate feedback cycle of terrestrial ecosystems (Luo et al., 2019; Jia et  
58 al., 2019; Li et al., 2020). The complexity, uncertainty, and large spatial heterogeneity  
59 of SOC stock estimation have limited the ability to accurately quantify the SOC stock  
60 distribution (Mishra et al., 2021; Wang et al., 2022a) To date, three main methods are  
61 commonly used to estimate large-scale SOC stocks: area-weighted averaging based  
62 on vegetation inventories and soil survey data (Tang et al., 2018), machine-learning  
63 based on remote-sensing, land-use, and edaphic data and climatic factors as covariates  
64 (Ding et al., 2016), and depth distribution function-based empirical analysis (Wang et  
65 al., 2023). The first approach provides the most accurate measurement of the SOC  
66 stock but is time-consuming and labor intensive and is not practical at the global  
67 scale. The latter two do not fully consider the vertical distribution of the soil profile or  
68 the soil properties of various ecosystems. The extrapolation to large soil depths, for  
69 example, using 0–40 cm or 0–50 cm of surface SOC to predict 0–100 cm or 0–200 cm  
70 of subsoil SOC (Wang et al., 2023; Ding et al., 2016), may lead to high uncertainty,  
71 thus preventing an accurate assessment of the global subsoil SOC stock.



72 Studies of whole-soil profiles have recorded greater changes in the SOC dynamics of  
73 the subsoil under warming (Zosso et al., 2023; Luo et al., 2020; Soong et al., 2021).  
74 The amount and quality of C in input soil, such as aboveground litter and root  
75 biomass input, could profoundly alter the vertical SOC distribution (Lange et al.,  
76 2023; Feng et al., 2022). The  $\beta$  model, in particular, uses simple and flexible functions  
77 that capture the relative slope of depth profiles with a single parameter, with the  
78 advantage of being able to integrate SOC values from the surface down to a given  
79 depth (Esteban G. Jobb gy. and Jackson., 2000). The  $\beta$  model was originally applied  
80 to vertical root distributions and has been used to fit the steepest reductions with depth  
81 (Gale and Grigal, 1987; Jackson et al., 1997). Some researchers have used the global  
82 average  $\beta$  of 0.9786 to calculate deep soil SOC stocks (Yang et al., 2011; Deng et al.,  
83 2014), however, the different hydrological conditions, soil type, and  
84 ground/underground organic matter have limited the ability to resolve the SOC depth  
85 distribution with confidence.

86 In this study, we produced spatially resolved global estimates of the depth distribution  
87 and stocks of subsoil SOC using the  $\beta$  model as a depth distribution function-based  
88 empirical approach for evaluating cropland, grassland, and forestland ecosystems on a  
89 global scale. First, we collected and analyzed 1221 soil profiles (0–1 m) of globally  
90 distributed observations from 478 sites to estimate the SOC vertical distribution (soil  
91  $\beta$  values). Then we developed a random forest (RF) model to estimate the spatial  
92 variation in grid-level soil  $\beta$  values in the associated ecosystems to resolve the  
93 dynamics of the SOC density in different soil layers and subsoil stocks of the global  
94 ecosystems.

95

## 96 **2. Methods**

### 97 **2.1. Data collection**

98 We conducted peer-reviewed literatures review of studies previously published on  
99 SOC stock or SOC content of soil profile between 1980 and 2022 to obtain a  
100 database. The Web of Science and China National Knowledge Infrastructure (CNKI)  
101 database were searched (article abstracts and key words) using the terms “Soil organic  
102 carbon” AND “subsoil” AND “Soil profile” AND “Deep soil” The criteria were as  
103 follows: (1) The research scope is worldwide, (2) the study was conducted in the field,  
104 (3) the profiles of multiple sites are reported in the same literature, and the profile of



105 each site is considered as an independent study, (4) profiles with more than three  
106 suitable measurements of organic carbon in the first meter were collected from the  
107 analysis for there was sufficient detail to characterize the vertical distribution of SOC,  
108 (5) the data extracted from included basic site information including location latitude  
109 and longitude, soil organic carbon (SOC), total nitrogen (TN), soil bulk density (BD),  
110 soil pH and C:N, Microbial biomass carbon and nitrogen (MC), Microbial biomass  
111 nitrogen (MN), and MC: MN, soil clay content, climate conditions [mean annual  
112 precipitation (MAP) and mean annual temperature (MAT)]. If the SOM rather than  
113 SOC was reported, the value was converted to SOC by multiplication with a  
114 conversion factor of 0.58 (Don et al., 2011). To extract data presented graphically, the  
115 digital software GetData Graph Digitizer 2.25 (getdata-graph-digitizer.com) was used.  
116 A total of 161 peer reviewed papers comprising 1221 soil profiles were included in  
117 this dataset, with the distribution of locations shown in Figure1. Missing soil and  
118 climate factor data from a few sites were either provided by the study authors through  
119 direct correspondence, or obtained from the spatial datasets (section 2.2), based on  
120 latitude and longitude. These data were analyzed to determine the impact of the  
121 environment on soil  $\beta$  values and develop a model to predict global grid-level  $\beta$   
122 values, subsequently, soil profiles SOC density, and calculate SOC stocks.

123

## 124 **2.2 Global soil attributes calculation**

125 Since the 0-1 m soil profile has different layers in the row data, mass-preserving  
126 spline method (R Package ‘mpspline2’) was used to divide the soil profiles into 5  
127 layers with 20 cm interval. This function implements for continuous down-profile  
128 estimates of soil attributes measured over discrete, often discontinuous depth  
129 intervals. In some studies, there was a lack of bulk density data below 20 cm soil  
130 layer. Notable differences in global SOC stocks estimations were attributed to the  
131 values used for soil bulk density. Therefore, we use the database issued by  
132 predecessors to generate bulk density data with 0-1m profile at 20 cm interval  
133 (Shangguan et al., 2014). For SOC density, it is necessary to supplement the bulk  
134 density data to calculate the SOC content. In order to reveal the variation of SOC  
135 dynamic with depth, we first have to calculate the SOC density (see Equation 1). The  
136 SOC stocks of each land use is equal to SOC density multiplied by its square (see  
137 Equation 2).

$$138 \text{ SOC density} = \text{SOC} * \text{BD} * D/10 \quad [1]$$

$$139 \text{ SOC stocks} = \text{SOC density} * S_{\text{ecosystem}} \quad [2]$$

140 where SOC is the SOC concentration ( $\text{g kg}^{-1}$ ), BD is the soil bulk density ( $\text{g cm}^{-3}$ ),  
141 and D is the thickness of the soil layer (at intervals of 20 cm in the first meter), SOC



142 density ( $\text{Mg C ha}^{-1}$ ).  $S_{\text{ecosystem}}$  is the areas of cropland, grassland or forestland (ha),  
143 SOC stocks ( $\text{Pg C}$ ).

### 144 **2.3 Global soil $\beta$ values calculation**

145 We obtained soil  $\beta$  data from 160 published studies representing 1221 observations.  
146 The original SOC density data the original soil depth available in individual study was  
147 converted to SOC density in the top 100 cm soil using the depth functions developed  
148 by Yang et al. (2011) according to the following equations:

$$149 \quad Y = 1 - \beta^d \quad [3]$$

$$150 \quad X_{100} = \frac{1 - \beta^{100}}{1 - \beta^{d_0}} * X_{d_0} \quad [4]$$

151 where Y represents the cumulative proportion of the SOC density from the soil  
152 surface to depth d (cm);  $\beta$  is the relative rate of decrease in the SOC density with soil  
153 depth;  $X_{100}$  denotes the SOC density in the upper 100 cm;  $d_0$  denotes in the 0-20 cm  
154 soil (cm); and  $X_{d_0}$  is the SOC density of the top 20 cm soil depth.

155

### 156 **2.4 Spatial gridded datasets**

157 The gridded datasets included forestland, grassland, and cropland areas, climate  
158 factors and soil properties. Areas of cropland, forestland, and grassland were obtained  
159 from Global Agro-Ecological Zones (GAEZ, <https://gaez.fao.org/>) at a resolution at  
160  $0.083^\circ \times 0.083^\circ$ . The MAP and MAT were acquired from the Climatic Research Unit  
161 Time Series (CRU TS ver. 4.05;  
162 [https://crudata.uea.ac.uk/cru/data/hrg/cru\\_ts\\_4.05/cruts.2103051243.v4.05/](https://crudata.uea.ac.uk/cru/data/hrg/cru_ts_4.05/cruts.2103051243.v4.05/)). The  
163 spatial SOC, total N, soil clay contents, and soil pH were acquired from the  
164 Harmonized World Soil Database ver. 1.2 ([https://www.fao.org/soils-portal/data-  
165 hub/soil-classification/worldreference-base/en/](https://www.fao.org/soils-portal/data-hub/soil-classification/worldreference-base/en/)). MC and MN data were obtained from  
166 this study (Xu et al., 2013). The BD dataset of the whole soil profile was acquired  
167 from gridded Global Soil Dataset for use in Earth System Models (GSDE)  
168 (<http://globalchange.bnu.edu.cn/research/soilw>), whose resolution is 30 arc-seconds.  
169 All data were resampled at  $0.083^\circ$  resolution using the “raster” R package  
170 (<https://rspatial.org/raster>).

171

### 172 **2.5 Application of RF modeling to predict global soil $\beta$ values**

173 We reconstruct the relationships among multiple factors, cropland, grassland and  
174 forestland soil  $\beta$  values by RF algorithm. The developed RF models were used to  
175 predict grid-level soil  $\beta$  values for each ecosystem. Prior to constructing the RF



176 model, the optimal parameter values of  $m_{try}$  and  $ntrees$  were determined through the  
177 bootstrap sampling method, which was performed with the “e1071” R package.  
178 Predictions of soil  $\beta$  values derived by RF and random-effects regression models were  
179 evaluated by 10-fold cross-validation. The dataset was divided into 10 subsets of  
180 equal size, of which 70% were used for model fitting and RF procedures, then  
181 predicted with the fitted models using the remaining 30% of the data. The  
182 performance of RF models was evaluated based on the coefficient of determination  
183 ( $R^2$ ) and root mean square error (RMSE) according to those following equations:

$$184 \quad R^2 = 1 - \frac{\sum_{p=1}^q (y_p - \hat{y}_p)^2}{\sum_{p=1}^q (y_p - \bar{y})^2} \quad [5]$$

185

$$186 \quad RMSE = \sqrt{\frac{\sum_{p=1}^q (y_p - \hat{y}_p)^2}{q}} \quad [6]$$

187 where  $y_p$  represents an observed value ( $p = 1, 2, 3, \dots$ ),  $\hat{y}_p$  represents the  
188 corresponding predicted value ( $p = 1, 2, 3, \dots$ ),  $\bar{y}$  represents the mean value of  
189 observed values, and  $q$  represents the total number of observed values.

190

## 191 **2.6 Data management and analyses**

192 One-way analysis of variance at  $p < 0.05$  was applied to identify significant  
193 differences in soil  $\beta$  values using SPSS ver. 20.0 (SPSS, Inc., Chicago, IL, USA)  
194 software. we made a database of peer-reviewed publications with Excel 2010 software  
195 (Microsoft Corp., Redmond, WA, USA). Weather data analyses were performed using  
196 MATLAB R2017a software (MathWorks Inc., Natick, MA, USA). Weather data were  
197 analyzed using MATLAB R2017a (MathWorks, Natick, MA, USA). Excel 2010, R  
198 software (ver. 3.5.1; R Development Core Team, Vienna, Austria) and SigmaPlot (ver.  
199 12.5; Systat Software Inc., San Jose, CA, USA) software were used to generate  
200 graphs. A publicly available map of China was obtained from the Resource and  
201 Environment Data Cloud Platform (<http://www.resdc.cn>). All map-related operations  
202 were implemented using ArcGIS 10.2 software (<http://www.esri.com/en-us/arcgis>). All  
203 algorithms implemented using the random Forest R package in the R software  
204 environment (ver. 3.5.1; R Development Core Team, Vienna, Austria).

205

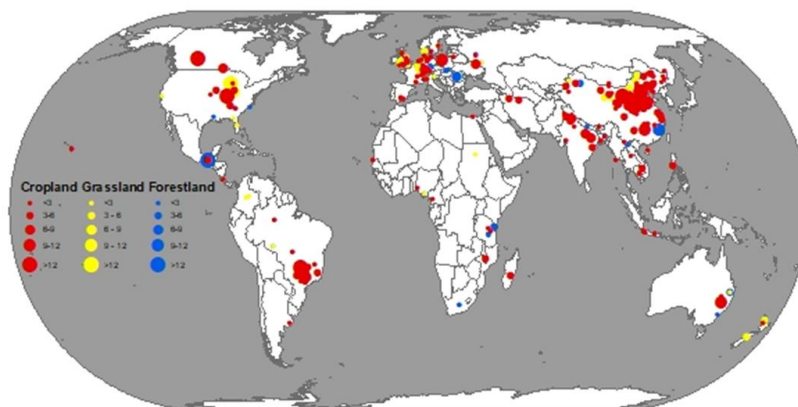
## 206 **3. Results**



207 **3.1 Soil  $\beta$  values of the three global ecosystems based on field measurements**

208 We analyzed 1221 observations (soil profile: 0–1 m): 758 for cropland, 219 for  
209 forestland, and 244 for grassland (Figure 1), we also quantified the magnitudes of  $\beta$   
210 (see Methods). Across all observations, the soil  $\beta$  values ranged from 0.9645 to 0.9831  
211 (5th–95th percentile), with a mean of 0.9756 and median of 0.9766. The average value  
212 was 0.9761, 0.9750, and 0.9743 for cropland, forestland, and grassland, respectively.  
213 The coefficients of variation (CVs) for the three ecosystems were as follows: forestland  
214 (CV: 0.72%) > grassland (CV: 0.71%) > cropland (CV: 0.54%). The significant  
215 differences in soil  $\beta$  values among the ecosystems were attributed to the different  
216 biological vegetation types (Figure S1).

217



218

219 **Figure 1.** Geographic location of the study sites included in the meta-analysis of the  
220 0–1 m soil profiles. The dot sizes reflect the sample sizes. Red, yellow, and blue dots  
221 represent cropland, grassland, and forestland, respectively.

222

223 **3.2 Impact of soil and climate variables on soil  $\beta$  values**

224 Nonparametric smooth regression was used to determine the direct and indirect  
225 relationships between the continuous explanatory variables and soil  $\beta$  values. Among  
226 the 13 explanatory variables, SOC, the ratio of SOC to soil total nitrogen (i.e., the C/N  
227 ratio), and the mean annual temperature (MAT) had the greatest influence on  $\beta$  values  
228 with relative contributions of 35%, 34%, and 28%. A higher MAT corresponded to

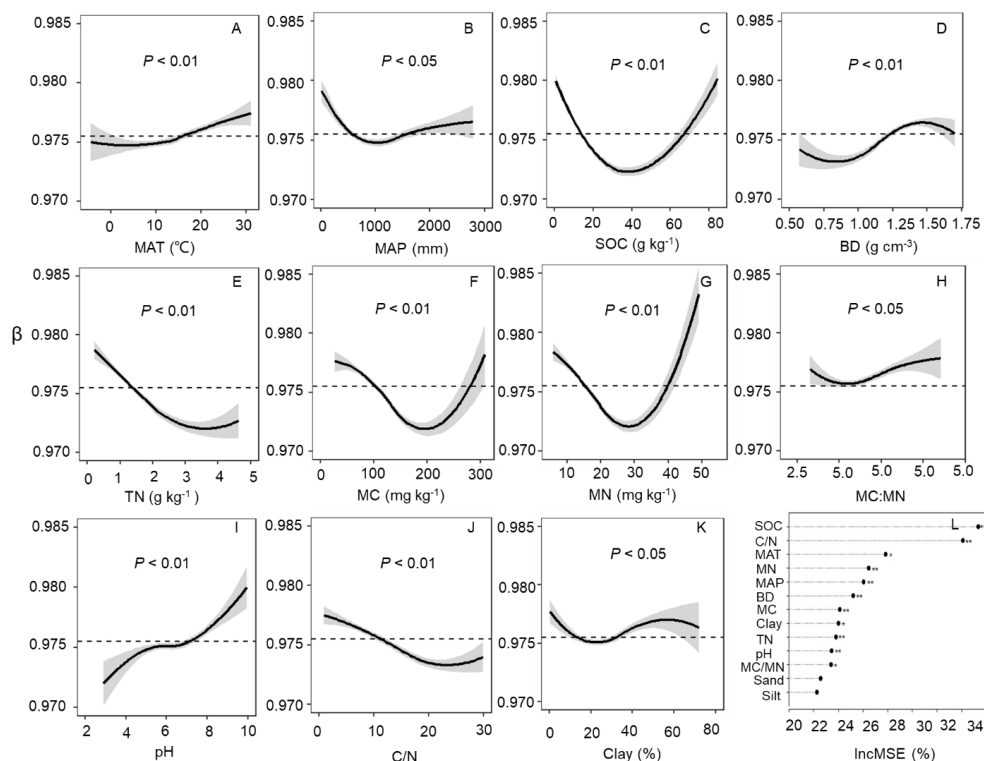




229 higher  $\beta$  values, particularly for MAT values greater than 20°C (Figure 2). The  $\beta$   
230 values decreased with an increase in mean annual precipitation (MAP) up to 1500 mm  
231 and increased when the MAP exceeded 1500 mm. These results indicate that higher  
232 temperatures and more precipitation promote the rapid decomposition of SOC into  
233 CO<sub>2</sub> from its sequestered state.

234 The effects of SOC, microbial biomass carbon (MC), and microbial biomass nitrogen  
235 (MN) on soil  $\beta$  values were strongly significant; the regression fittings of these  
236 variables were open downward parabolic, with peaks at about 40 g kg<sup>-1</sup>, 200 mg kg<sup>-1</sup>,  
237 and 30 mg kg<sup>-1</sup>, respectively. With increases in the topsoil SOC, MC, and MN, the  $\beta$   
238 values first decreased and then increased. The MC:MN ratio indicated a relatively  
239 weak but significant positive effect on  $\beta$  values. The  $\beta$  values decreased with  
240 increases in soil total nitrogen (TN) and the C/N ratio, indicating that C in the soil is  
241 more likely to be sequestered under high N or a high C/N ratio; the relative rate of  
242 decline of the SOC density decreased with increasing depth. A sharp increase was  
243 observed at pH < 6 or >8, whereas the  $\beta$  value remained stable for pH levels between  
244 6 and 8. Thus, within a reasonable soil pH range, the relative rate of decline in the  
245 SOC density with depth tended to be stable. The clay content of the soil had no  
246 significant influence on the soil  $\beta$  value.

247



248

249 **Figure 2.** Plots A–K show the variables affecting soil  $\beta$  values. MAT, mean annual  
 250 temperature; MAP, mean annual precipitation; SOC, soil organic carbon; BD, bulk  
 251 density; TN, soil total nitrogen; MC, microbial biomass carbon; MN, microbial  
 252 biomass nitrogen; C/N, soil organic carbon/soil total nitrogen; Clay, soil clay content.  
 253 Shaded bands indicate 95% confidence intervals, and the dashed lines represent the  
 254 average soil  $\beta$  values. Relative contributions of the factors to soil  $\beta$  values (L).

255

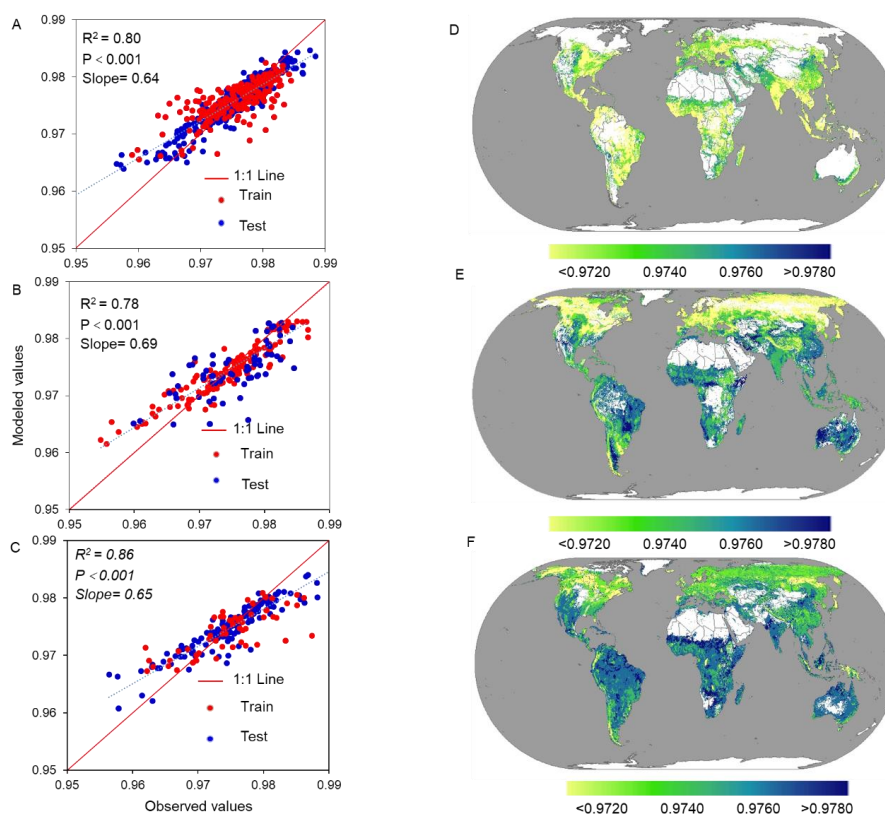
### 256 3.3 Performance of the random forest regression model

257 We developed an RF regression model using machine learning techniques to  
 258 determine grid-level soil  $\beta$  values on a global scale. The model included 11 significant  
 259 factors (SOC, C/N, MAT, MN, MAP, BD, MC, Clay, TN, pH, MC:MN), as well as  
 260 the corresponding high-spatial-resolution raster datasets (Figures S2–S4). The model  
 261 performed well, with an adjusted coefficient of determination ( $R^2$ ) of 0.80, 0.78, and  
 262 0.86 for cropland, grassland, and forestland, respectively (Figure 3). The predictions



263 and measurements of all samples were also distributed close to the 1:1 line. These  
264 validations suggest that the trained RF model is capable of capturing and predicting  
265 the spatial pattern of the soil  $\beta$  value on a global scale.

266



267

268 **Figure 3.** Grid-level maps showing the predicted global soil  $\beta$  values. Plots A–C  
269 reflect the performance of the random forest model as evaluated by the correlation  
270 between the observed and predicted responses of soil  $\beta$  values. Plots D–F represent  
271 the spatial variability of soil  $\beta$  values in cropland, grassland, and forestland,  
272 respectively.

273

### 274 **3.4 Mapping the global grid-level soil $\beta$ value**

275 We predicted the global soil  $\beta$  value using the RF model for 4,057,524 integrated



276 grid-level, high-spatial-resolution soil and climate raster datasets (cropland,  $n =$   
277 832,827; forestland,  $n = 1,695,053$ ; and grassland,  $n = 1,529,644$ ). The average value  
278 was 0.9727, 0.9739, and 0.9751 for cropland, grassland, and forestland, respectively,  
279 with CVs of 0.2%, 4.4%, and 3.8%. More than 95% of the grids were less than that ( $\beta$   
280 = 0.9786) reported by the reference (Esteban G. Jobbágy. and Jackson., 2000). The  
281 results of the predicted soil  $\beta$  indicate that the relative rate of decline of SOC stocks  
282 was highest for forestland, followed by grassland and cropland.

283 There was extensive geographic variability in soil  $\beta$  values according to land use. In  
284 central North America, cropland, grassland and forestland all had high  $\beta$  values  
285 (Figure 3). The large  $\beta$  values for cropland were distributed in Sub-Saharan Africa,  
286 central North America, and southern Oceania. The large  $\beta$  values for grassland were  
287 distributed mainly in eastern and southern South America and Oceania. For  
288 forestland, the large  $\beta$  values were mainly distributed in northern South America,  
289 central and southern Africa, Oceania (except for the central region), and northeastern  
290 Africa. The low values exhibited similar spatial patterns among land uses and were  
291 found mainly in northern and western regions of Europe and in northern and eastern  
292 regions of North America.

293

### 294 ***3.5 Spatial variability of the soil organic carbon (SOC) density in subsoil (20–100*** 295 ***cm soil layer)***

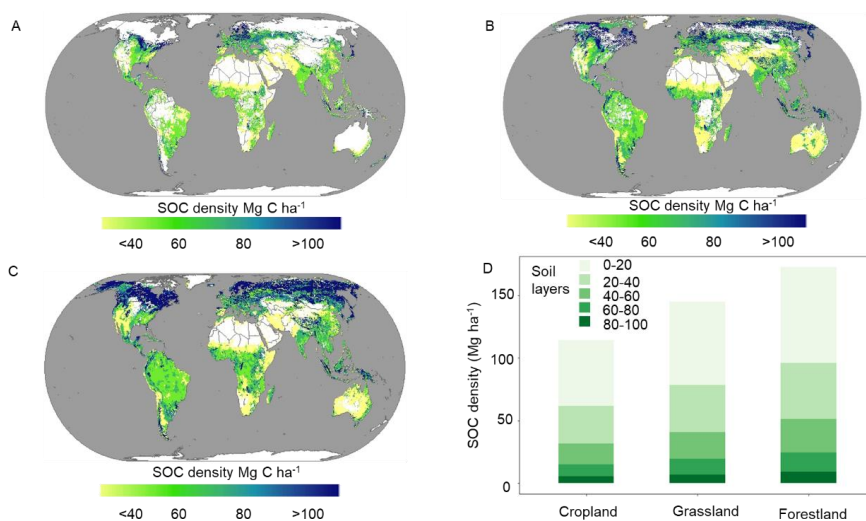
296 The estimated values for the global average SOC density of cropland, grassland, and  
297 forestland were 63.8, 83.3, and 100.4 Mg ha<sup>-1</sup>, respectively, for the 20–100 cm layer  
298 (Table S1), with considerable spatial variation on the global scale (Figure 4). The  
299 larger the soil  $\beta$  value, the more rapidly the SOC density decreased with an increase in  
300 soil depth. Spatially, there was geographic variability in the density depending on  
301 ecosystems. The higher values exhibited similar spatial patterns in each ecosystems  
302 type and were distributed mainly in northern and western Europe and northern and  
303 eastern North America. The highest SOC density and microbial C/N ratios were found  
304 at high latitudes in tundra and boreal forests, probably due to the higher levels of  
305 organic matter in soils, greater fungal abundance, and lower nutrient availability in  
306 cold biomes (Gao et al., 2022).

307 For cropland, the lower values were distributed in eastern and southwestern Asia,



308 Sub-Saharan Africa, southern Africa, central North America, and southern Oceania.  
309 For grassland, the lower values were mainly distributed in eastern and southwestern  
310 Asia, eastern, and southern South America, and Oceania. For forestland, the lower  
311 values were mainly distributed in northern South America, central, and southern  
312 Africa, the central most region of Oceania, and northeastern Africa. The spatial  
313 variation in SOC density at multiple standardized depths (20–40, 40–60, 60–80, and  
314 80–100 cm) was also estimated (Figures S5–S7), which exhibited a decreasing trend  
315 with increasing depth. The global subsoil SOC stock was estimated to be 912 Pg C,  
316 being 67, 200, and 644 Pg C in cropland, grassland, and forestland (Table 1). Subsoil  
317 contains more SOC stock; the subsoils of cropland, grassland, and forestland stored 9,  
318 30, and 125 Pg (Table 1) more than the topsoil, respectively. In addition, soil at  
319 depths of 20–100 cm beneath the surface contained on average 54% of the topsoil at  
320 0–100 cm.

321



322

323 **Figure 4.** Grid-level maps showing the predicted global subsoil SOC density for the  
324 20–100 cm soil layer. A–C represents cropland, grassland, and forestland,  
325 respectively. D shows the SOC density in soil profiles of cropland, grassland, and  
326 forestland.

327

328 **4. Discussion**



329 **4.1 Comparison of high-resolution SOC dynamics**

330 Global SOC stock estimations reported in the literature vary considerably. For SOC  
331 stock, the estimated cropland, grassland and forestland (Table 1) were very close to  
332 the previous studies (Liu et al., 2021; Conant, 2010; Dixon et al., 1994). It indicated  
333 that our method is feasible and the estimation is relatively correct. The subsoil SOC  
334 stock of all land for the 0–100 cm soil layer (Table 1), which was slightly lower than  
335 the result of that (Sanderman et al., 2017) but higher compared to the commonly used  
336 range of 1462–1548 Pg C (Batjes, 1996) and other research results (Scharlemann et  
337 al., 2014; Roland Hiederer. and Köchy., 2011; Georgiou et al., 2022). The result of  
338 that (Sanderman et al., 2017) may be overestimated, mainly because of the training  
339 dataset used to build spatial predictions models was not ideal ( $R^2=0.54$ ) for testing the  
340 hypotheses. Overall, we believe that our value is not an overestimate, as previous  
341 estimates (Batjes, 1996) used a database containing very few soil profiles from North  
342 America, Oceania, or the north temperate regions (Scharlemann et al., 2014)  
343 We found that the subsoil contains an average of 54% of the top 0–100 cm soil's SOC  
344 stock, which is consistent with the percentages cited in previous works (47–55%)  
345 (Lal, 2018; Balesdent et al., 2018). Subsoil contains more SOC stock, which has  
346 greater potential for C sequestration. Our estimated SOC density (Table S1) for  
347 cropland was slightly higher than that reported in other study (Liu et al., 2021) , and  
348 lower than that of tropical cropland (Reichenbach et al., 2023). For forestland, it was  
349  $180.6 \text{ Mg ha}^{-1}$  overall, consistent with that (Dixon et al., 1994) but much lower than  
350 that of mangroves and tropical forestland (Atwood et al., 2017; Reichenbach et al.,  
351 2023). For grassland, it was  $153.7 \text{ Mg ha}^{-1}$  overall, much higher than that of (Conant  
352 et al., 2017). Finally, globally, it was  $150.9 \text{ Mg ha}^{-1}$  overall, much higher than that of  
353 the research (Roland Hiederer. and Köchy., 2011)

354

355



356

357 Table 1. Comparisons of the estimated SOC density with other studies

	Global area (10 <sup>9</sup> ha)	Topsoil (Pg) 0–30 (0–20) (cm)	Subsoil (Pg) 30–100 (20–100) (cm)	Total (Pg) 0–100 (cm)	References
Cropland		58	69	127	(Liu et al., 2021)
Cropland	1.20	58	67	125	This study
Forestland	4.1	359	787	1146	(Dixon et al., 1994)
Forestland	5.64	519	644	1164	This study
Grassland				343	(Conant, 2010)
Grassland	2.59	170	200	370	This study
All land		684–724	778–824	1462–1548	(Batjes, 1996)
All land		699	718	1417	(Roland Hiederer. and Köchy., 2011)
All land		699	716	1416	(Scharlemann et al., 2014)
All land		863	961	1824	(Sanderman et al., 2017)
All land		748	912	1659	This study

358 SOC: soil organic carbon.

359

#### 360 **4.2 Factors affecting soil $\beta$**

361 Climatic factors and soil properties had significant effects on soil  $\beta$  values. MAT was  
 362 significantly positively correlated with soil  $\beta$ ; specifically, the higher the MAT, the  
 363 faster the SOC density decreased with depth. In agreement with our result, SOC  
 364 stocks declines strongly with MAT by analyzing >9,000 soil profiles (Hartley et al.,  
 365 2021). The change in SOC stock was nonlinear and negative with respect to MAT,  
 366 high rates of SOC decomposition occur with high temperatures when MAT exceeded  
 367 19 °C (Zhao et al., 2013). In the current study, MAP had a significant effect on the  
 368 SOC density, with a threshold of 1,500 mm. Above the threshold, SOC may  
 369 decompose; below the threshold, it tended to remain sequestered. In wetter climates  
 370 where the precipitation exceeds evapotranspiration, there is a strong relationship  
 371 between mineral-associated SOC concentration and persistence, due to the humid soil  
 372 environments that favor greater root growth and abundance (Heckman et al., 2023).

373 Our results highlight the important role of edaphic properties in explaining variation  
 374 in mean soil  $\beta$  values, as opposed to climate alone (Figure 2). When the C/N ratio is  
 375 high, more SOC migrates downward; however, the SOC content decreases rapidly



376 with depth. Under a soil C/N ratio > 15, warming significantly enhances the  
377 development of root biomass (Bai et al., 2023), this could induce a corresponding  
378 SOC accumulation, such that the soil  $\beta$  values would trend downward. Our results  
379 showed that for near-neutral pH soils, the  $\beta$  values did not significantly change; thus,  
380 in this case, there is a greater potential for soil C storage through increased microbial  
381 growth efficiency and greater channeling of substrates into biomass synthesis. By  
382 contrast, in acidic soils, microbial growth is a bigger constraint on the decomposition  
383 rate, leading to large losses of carbon (Malik et al., 2018). Soil pH had non-linear  
384 relationships with microorganisms, tends to be neutral, and the abundance of  
385 microorganisms is higher (Patoine et al., 2022). Microbial necromass was a major  
386 source for SOC formation in global ecosystems (Wang et al., 2021a).

387 The effects of MC, MN, and SOC on soil  $\beta$  values exhibited the same trend. MC had  
388 positive relationships with the SOC content across the large spatial scale, because of  
389 microbes should be considered not only as a controlling factor of the consumption of  
390 SOC, but also as an influencing factor of the production of SOC (Tao et al., 2023). In  
391 the current study, MC and MN concentrations were most closely linked to SOC,  
392 whereas climatic factors were most important for stoichiometry in microbial biomass  
393 ratios. Evidence from China shows that microbial residues contribute a larger  
394 proportion of SOC in subsoils than in topsoil (Wen et al., 2023). TN content, labile  
395 and recalcitrant C components, and soil water content contributed the most to SOC  
396 sequestration, which was attributed to differences in plant litter, root biomass input,  
397 and hydrological conditions (Xia et al., 2021)

398

#### 399 ***4.3 Challenges and opportunities: Deep soil SOC sequestration***

400 More and more studies have shown about the necessity to better understand subsoil  
401 SOC dynamics. Biotic controls on SOC cycling become weaker as mineral controls  
402 predominate with depth (Hicks Pries et al., 2023). The topsoil is rich in carbohydrates  
403 and lignin, while the subsoil is rich in protein and lipids, the decrease rate of the ratio  
404 of the microbially derived C to plant-derived C with SOM content was 23%–30%  
405 slower in the subsoil than in the topsoil (Huang et al., 2023). Warming stimulates  
406 microbes metabolic activities for structurally complex organic carbon, resulting Large  
407 loss of subsoil polymeric SOC than topsoil (Zosso et al., 2023). However, long-term  
408 experiments may not be long enough to quantify SOC dynamics in subsoil, large-





409 scale research methods and machine learning are particularly important and  
410 necessary. Based on measured soil profile data and environmental variables, Wang et  
411 al. combined with machine learning methods to assess SOC storage and spatial  
412 distribution of subsoil in frozen soil areas in the third pole region (Wang et al.,  
413 2021b). The process of studying deep soil organic carbon is complex, the experiments  
414 manipulate are difficult and time-consuming, which leads to a small amount of  
415 research data, which lead model-derived predictions contain large uncertainties. To  
416 avoid under- or overestimation of the SOC stocks of an ecosystem, it is important to  
417 consider the subsoil when formulating sequestration policies for the whole soil profile  
418 (Button et al., 2022), as the “4 per 1000” approach for the top 30 to 40 cm soil layer  
419 provides an incomplete representation of the soil profile (Rumpel et al., 2018). It may  
420 be essential to sample the soil deeper (e.g. 0–100cm) and incorporate deep soils into  
421 future manipulations, measurements and models.

422 In addition, researchers had quantified the contribution of optimizing crop  
423 redistribution and improved management, and topsoil carbon sequestration in  
424 offsetting anthropogenic GHG emissions and climate change (Wang et al., 2022b;  
425 Rodrigues et al., 2021; Yulong Yin et al., 2023), the ability and consequence of  
426 subsoil SOC sequestration of crop management remains to be further studied.  
427 Conducting global-scale subsoil SOC dynamics studies will fill the knowledge gap to  
428 develop appropriate soil C sequestration strategies and policies to help the world cope  
429 with climate change and food security (Amelung et al., 2020; Bossio et al., 2020). As  
430 such, it is crucial that future research efforts focus on SOC sequestration efficiency  
431 with climate change, considering the entire soil profile.

432

#### 433 ***4.4 Strengths and limitations***

434 Our research provides a scientific foundation for further study of SOC dynamics,  
435 sequestration, and emissions reduction across soil profiles, and have some  
436 implications for meeting Sustainable Development Goals (SDGs), especially SDG2  
437 Zero hunger, SDG13 Climate action, and SDG15 Life on land  
438 (<https://www.undp.org/sustainable-development-goals>). To the best of our knowledge,  
439 this study presents the first global high-resolution maps of the spatial pattern of soil  
440 profile SOC density derived from soil  $\beta$  values driven by soil properties and climate.  
441 We found that there were great differences in the dynamics of SOC density among



442 different land types, in which forestland showed the highest density followed by  
443 grassland and cropland. However, differences in SOC dynamics between the  
444 investigated soils was mainly due to the dominant biogeochemical properties of the  
445 soil, rather than land use (Reichenbach et al., 2023). Our study considered the effects  
446 of multiple environmental variables (climatic factors, soil physicochemical  
447 properties), and different ecosystems on subsoil SOC dynamics. The decline in SOC  
448 density across the profiles varies greatly with depth in most areas, suggesting that  
449 action should be taken to improve soil management in these areas. Our results  
450 emphasize the importance of implementing policies that improve the carbon  
451 sequestration potential of deep soil, as this may also lead to improved soil fertility and  
452 reduced greenhouse gas emissions. In the future, it is necessary to explore the carbon  
453 sequestration mechanism and carbon turnover time below the surface layer, so as to  
454 better understand and estimate deep SOC stocks.

455 Some important aspects of SOC stocks were not included in this study. For instance,  
456 microbial necromass is an essential factor in SOC accrual (Zhou et al., 2023),  
457 however, to date, although included to some extent in meta-analysis studies, reliable  
458 global-scale estimations are lacking. Due to difficulties in obtaining management data  
459 for grasslands and forestlands, we did not consider possible specific management  
460 factors on soil  $\beta$  value estimations. For example, N fertilizer application, irrigation  
461 amount, soil tillage practices, and organic carbon inputs (straw returning, crop  
462 residues, and litterfall) may affect SOC vertical movement. Moreover, organic carbon  
463 inputs can modify SOC decomposition rates, particularly at deep soil depths  
464 (Cardinael et al., 2018). These shortcomings can only be overcome by obtaining and  
465 analyzing more detailed data on soil and climate characteristics, and developing more  
466 sophisticated modeling methods.

467

## 468 **5. Data availability**

469 The data of “global patterns of soil organic carbon dynamics in the 20–100 cm soil  
470 profile for different ecosystems: a global meta-analysis” are available at  
471 <https://doi.org/10.5281/zenodo.10846543> (Wang et al., 2024). The file name is  
472 “GE\_β.tif”, GE represents global ecosystems, which including cropland(CL),  
473 grassland(GL), and forestland(FL). “FL\_β.tif” represents the spatial distribution of  $\beta$



474 for forestland at 20-100 cm depth. The file name is “GE\_d\_SOCD.tif”, where SOCD  
475 represents soil organic carbon density, d represents soil depth, for example, “FL\_20-  
476 100\_SOCD.tif” represents the spatial distribution of SOCD for forestland at 20-100  
477 cm depth.

478

## 479 **6. Conclusion**

480 Accurately quantifying the distribution of soil profile SOC stocks is crucial for C  
481 sequestration and mitigation. Herein, machine learning was applied to the  $\beta$  model to  
482 estimate SOC stocks in 20–100 cm depth soil profiles. The subsoil SOC density  
483 values of cropland, grassland, and forestland were estimated to be 63.8, 83.3, and  
484 100.4 Mg ha<sup>-1</sup>, respectively, and there was extensive geographic variability under  
485 different ecosystems. Moreover, the global subsoil SOC stocks of cropland, grassland,  
486 and forestland were 67, 200, and 644 Pg C. In summary, the dataset can be used to  
487 modify existing Earth system models and improve prediction accuracy, as well as also  
488 elucidate global SOC dynamics and variability in spatial patterns in whole soil  
489 profiles and provides a reference for decision makers to develop more effective  
490 carbon budget management strategies.

491

## 492 **Author contributions**

493 The study was completed with cooperation between all authors. ZC and YY  
494 conceived and designed the research. HW: conceptualization, investigation,  
495 methodology, data curation, visualization, conducted data analysis and wrote original  
496 draft. XT: methodology, data curation, visualization, TC: investigation, data curation,  
497 conceptualization, investigation. ZC, KH, ZW, HG, QM, YW, YC, MZ contributed to  
498 the scientific discussions. ZC and QZ: conceptualization, supervision, funding  
499 acquisition.

500

501 **Competing interests.** The authors declare that they have no conflict of interest

502



503 **Disclaimer. Publisher's note:** Copernicus Publications remains neutral with regard to  
504 jurisdictional claims in published maps and institutional affiliations.

505

506 **Acknowledgements.** This work was financially supported by the PhD Scientific  
507 Research and Innovation Foundation of Sanya Yazhou Bay Science and Technology  
508 City (HSPHDSRF-2022-05-013), and the Hainan Provincial Joint Project of Sanya  
509 Yazhou Bay Science and Technology City (2021JJLH0015), and the National Key  
510 Research and Development Program of China (2021YFD1900901).

511

512 **Financial support.** This work was supported by the PhD Scientific Research and  
513 Innovation Foundation of Sanya Yazhou Bay Science and Technology City  
514 (HSPHDSRF-2022-05-013), and the Hainan Provincial Joint Project of Sanya Yazhou  
515 Bay Science and Technology City (2021JJLH0015), and the National Key Research  
516 and Development Program of China (2021YFD1900901).



517 **References**

518

519 Amelung, W., Bossio, D., de Vries, W., Kögel-Knabner, I., Lehmann, J., Amundson, R.,

520 Bol, R., Collins, C., Lal, R., Leifeld, J., Minasny, B., Pan, G., Paustian, K., Rumpel, C.,

521 Sanderman, J., van Groenigen, J. W., Mooney, S., van Wesemael, B., Wander, M., and

522 Chabbi, A.: Towards a global-scale soil climate mitigation strategy, *Nature*

523 *Communications*, 11, 5427, 10.1038/s41467-020-18887-7, 2020.

524 Atwood, T. B., Connolly, R. M., Almahsheer, H., Carnell, P. E., Duarte, C. M., Ewers

525 Lewis, C. J., Irigoien, X., Kelleway, J. J., Lavery, P. S., Macreadie, P. I., Serrano, O.,

526 Sanders, C. J., Santos, I., Steven, A. D. L., and Lovelock, C. E.: Global patterns in

527 mangrove soil carbon stocks and losses, *Nature Climate Change*, 7, 523-528,

528 10.1038/nclimate3326, 2017.

529 Bai, T., Wang, P., Qiu, Y., Zhang, Y., and Hu, S.: Nitrogen availability mediates soil

530 carbon cycling response to climate warming: A meta-analysis, *Global Change Biology*,

531 29, 2608-2626, <https://doi.org/10.1111/gcb.16627>, 2023.

532 Balesdent, J., Basile-Doelsch, I., Chadoeuf, J., Cornu, S., Derrien, D., Fekiacova, Z.,

533 and Hatté, C.: Atmosphere–soil carbon transfer as a function of soil depth, *Nature*, 559,

534 599-602, 10.1038/s41586-018-0328-3, 2018.

535 Batjes, N. H.: Total carbon and nitrogen in the soils of the world, *European Journal of*

536 *Soil Science*, 47, 151-163, 10.1111/j.1365-2389.1996.tb01386.x, 1996.

537 Beillouin, D., Corbeels, M., Demenois, J., Berre, D., Boyer, A., Fallot, A., Feder, F.,

538 and Cardinael, R.: A global meta-analysis of soil organic carbon in the Anthropocene,

539 *Nat Commun*, 14, 3700, 10.1038/s41467-023-39338-z, 2023.

540 Bossio, D. A., Cook-Patton, S. C., Ellis, P. W., Fargione, J., Sanderman, J., Smith, P.,

541 Wood, S., Zomer, R. J., von Unger, M., Emmer, I. M., and Griscom, B. W.: The role of

542 soil carbon in natural climate solutions, *Nature Sustainability*, 3, 391-398,

543 10.1038/s41893-020-0491-z, 2020.

544 Bradford, M. A., Wieder, W. R., Bonan, G. B., Fierer, N., Raymond, P. A., and Crowther,

545 T. W.: Managing uncertainty in soil carbon feedbacks to climate change, *Nature Climate*

546 *Change*, 6, 751-758, 10.1038/nclimate3071, 2016.



- 547 Cardinael, R., Guenet, B., Chevallier, T., Dupraz, C., Cozzi, T., and Chenu, C.: High  
548 organic inputs explain shallow and deep SOC storage in a long-term agroforestry  
549 system – combining experimental and modeling approaches, *Biogeosciences*, 15, 297-  
550 317, 10.5194/bg-15-297-2018, 2018.
- 551 Chabbi, A., Lehmann, J., Ciais, P., Loescher, H. W., Cotrufo, M. F., Don, A.,  
552 SanClements, M., Schipper, L., Six, J., Smith, P., and Rumpel, C.: Aligning agriculture  
553 and climate policy, *Nature Climate Change*, 7, 307-309, 10.1038/nclimate3286, 2017.
- 554 Chen, J., Luo, Y., and Sinsabaugh, R. L.: Subsoil carbon loss, *Nature Geoscience*, 16,  
555 284-285, 10.1038/s41561-023-01164-9, 2023.
- 556 Conant, R. T.: Challenges and opportunities for carbon sequestration in grassland  
557 systems: a technical report on grassland management and climate change mitigation,  
558 Conant, R. T., Cerri, C. E. P., Osborne, B. B., and Paustian, K.: Grassland management  
559 impacts on soil carbon stocks: a new synthesis, *Ecological Applications*, 27, 662-668,  
560 <https://doi.org/10.1002/eap.1473>, 2017.
- 561 Deng, L., Liu, G. B., and Shangguan, Z. P.: Land-use conversion and changing soil  
562 carbon stocks in China's 'Grain-for-Green' Program: a synthesis, *Glob Chang Biol*, 20,  
563 3544-3556, 10.1111/gcb.12508, 2014.
- 564 Ding, J., Li, F., Yang, G., Chen, L., Zhang, B., Liu, L., Fang, K., Qin, S., Chen, Y., Peng,  
565 Y., Ji, C., He, H., Smith, P., and Yang, Y.: The permafrost carbon inventory on the  
566 Tibetan Plateau: a new evaluation using deep sediment cores, *Glob Chang Biol*, 22,  
567 2688-2701, 10.1111/gcb.13257, 2016.
- 568 Dixon, R. K., Solomon, A. M., Brown, S., Houghton, R. A., Trexler, M. C., and  
569 Wisniewski, J.: Carbon Pools and Flux of Global Forest Ecosystems, *Science*, 263, 185-  
570 190, doi:10.1126/science.263.5144.185, 1994.
- 571 Don, A., Schumacher, J., and Freibauer, A.: Impact of tropical land-use change on soil  
572 organic carbon stocks – a meta-analysis, *Global Change Biology*, 17, 1658-1670,  
573 <https://doi.org/10.1111/j.1365-2486.2010.02336.x>, 2011.
- 574 Esteban G. Jobbágy. and Jackson, R. B.:  
575 The vertical distribution of soil organic carbon and its relation to climate and vegetati  
576 on, *Ecological applications*, 10, 423-436, 10.1890/1051-0761, 2000.



- 577 Feng, J., He, K., Zhang, Q., Han, M., and Zhu, B.: Changes in plant inputs alter soil  
578 carbon and microbial communities in forest ecosystems, *Glob Chang Biol*, 28, 3426-  
579 3440, [10.1111/gcb.16107](https://doi.org/10.1111/gcb.16107), 2022.
- 580 Gale, M. R. and Grigal, D. F.: Vertical root distributions of northern tree species in  
581 relation to successional status, *Canadian Journal of Forest Research*, 17, 10.1139/x87-  
582 131, 1987.
- 583 Gao, D., Bai, E., Wang, S., Zong, S., Liu, Z., Fan, X., Zhao, C., and Hagedorn, F.:  
584 Three-dimensional mapping of carbon, nitrogen, and phosphorus in soil microbial  
585 biomass and their stoichiometry at the global scale, *Global Change Biology*, 28, 6728-  
586 6740, <https://doi.org/10.1111/gcb.16374>, 2022.
- 587 Georgiou, K., Jackson, R. B., Vindušková, O., Abramoff, R. Z., Ahlström, A., Feng, W.,  
588 Harden, J. W., Pellegrini, A. F. A., Polley, H. W., Soong, J. L., Riley, W. J., and Torn,  
589 M. S.: Global stocks and capacity of mineral-associated soil organic carbon, *Nature*  
590 *Communications*, 13, 3797, [10.1038/s41467-022-31540-9](https://doi.org/10.1038/s41467-022-31540-9), 2022.
- 591 Griscom, B. W., Adams, J., Ellis, P. W., Houghton, R. A., Lomax, G., Miteva, D. A.,  
592 Schlesinger, W. H., Shoch, D., Siikamaki, J. V., Smith, P., Woodbury, P., Zganjar, C.,  
593 Blackman, A., Campari, J., Conant, R. T., Delgado, C., Elias, P., Gopalakrishna, T.,  
594 Hamsik, M. R., Herrero, M., Kiesecker, J., Landis, E., Laestadius, L., Leavitt, S. M.,  
595 Minnemeyer, S., Polasky, S., Potapov, P., Putz, F. E., Sanderman, J., Silvius, M.,  
596 Wollenberg, E., and Fargione, J.: Natural climate solutions, *Proc Natl Acad Sci U S A*,  
597 114, 11645-11650, [10.1073/pnas.1710465114](https://doi.org/10.1073/pnas.1710465114), 2017.
- 598 Hartley, I. P., Hill, T. C., Chadburn, S. E., and Hugelius, G.: Temperature effects on  
599 carbon storage are controlled by soil stabilisation capacities, *Nature Communications*,  
600 12, 6713, [10.1038/s41467-021-27101-1](https://doi.org/10.1038/s41467-021-27101-1), 2021.
- 601 Heckman, K. A., Possinger, A. R., Badgley, B. D., Bowman, M. M., Gallo, A. C., Hatten,  
602 J. A., Nave, L. E., SanClements, M. D., Swanston, C. W., Weiglein, T. L., Wieder, W.  
603 R., and Strahm, B. D.: Moisture-driven divergence in mineral-associated soil carbon  
604 persistence, *Proceedings of the National Academy of Sciences*, 120, e2210044120,  
605 [doi:10.1073/pnas.2210044120](https://doi.org/10.1073/pnas.2210044120), 2023.
- 606 Hicks Pries, C. E., Ryals, R., Zhu, B., Min, K., Cooper, A., Goldsmith, S., Pett-Ridge,



- 607 J., Torn, M., and Berhe, A. A.: The Deep Soil Organic Carbon Response to Global  
608 Change, *Annual Review of Ecology, Evolution, and Systematics*, 54, 375-401,  
609 10.1146/annurev-ecolsys-102320-085332, 2023.
- 610 Huang, W., Kuzyakov, Y., Niu, S., Luo, Y., Sun, B., Zhang, J., and Liang, Y.: Drivers of  
611 microbially and plant-derived carbon in topsoil and subsoil, *Glob Chang Biol*, 29, 6188-  
612 6200, 10.1111/gcb.16951, 2023.
- 613 Jackson, R. B., Mooney, H. A., and Schulze, E. D.: A global budget for fine root biomass,  
614 surface area, and nutrient contents, *Proceedings of the National Academy of Sciences*,  
615 94, 7362-7366, 10.1073/pnas.94.14.73, 1997.
- 616 Jia, J., Cao, Z., Liu, C., Zhang, Z., Lin, L., Wang, Y., Haghypour, N., Wacker, L., Bao,  
617 H., Dittmar, T., Simpson, M. J., Yang, H., Crowther, T. W., Eglinton, T. I., He, J. S., and  
618 Feng, X.: Climate warming alters subsoil but not topsoil carbon dynamics in alpine  
619 grassland, *Glob Chang Biol*, 25, 4383-4393, 10.1111/gcb.14823, 2019.
- 620 Lal, R.: Digging deeper: A holistic perspective of factors affecting soil organic carbon  
621 sequestration in agroecosystems, *Global Change Biology*, 24, 3285 - 3301, 2018.
- 622 Lal, R.: Managing soils for negative feedback to climate change and positive impact on  
623 food and nutritional security, *Soil Science and Plant Nutrition*, 66, 1-9,  
624 10.1080/00380768.2020.1718548, 2020.
- 625 Lal, R., Monger, C., Nave, L., and Smith, P.: The role of soil in regulation of climate,  
626 *Philos Trans R Soc Lond B Biol Sci*, 376, 20210084, 10.1098/rstb.2021.0084, 2021.
- 627 Lange, M., Eisenhauer, N., Chen, H., and Gleixner, G.: Increased soil carbon storage  
628 through plant diversity strengthens with time and extends into the subsoil, *Glob Chang*  
629 *Biol*, 29, 2627-2639, 10.1111/gcb.16641, 2023.
- 630 Li, J. Q., Pei, J. M., Pendall, E., Reich, P. B., Noh, N. J., Li, B., Fang, C. M., and Nie,  
631 M.: Spatial heterogeneity and environmental predictors of permafrost region soil  
632 organic carbon stocks, *Science Advances*, 7, 10.1002/adv.202001242, 2020.
- 633 Liu, Y., Ge, T., van Groenigen, K. J., Yang, Y., Wang, P., Cheng, K., Zhu, Z., Wang, J.,  
634 Li, Y., Guggenberger, G., Sardans, J., Penuelas, J., Wu, J., and Kuzyakov, Y.: Rice paddy  
635 soils are a quantitatively important carbon store according to a global synthesis,  
636 *Communications Earth & Environment*, 2, 10.1038/s43247-021-00229-0, 2021.





- 637 Luo, Z., Wang, G., and Wang, E.: Global subsoil organic carbon turnover times  
638 dominantly controlled by soil properties rather than climate, *Nat Commun*, 10, 3688,  
639 10.1038/s41467-019-11597-9, 2019.
- 640 Luo, Z., Luo, Y., Wang, G., Xia, J., and Peng, C.: Warming-induced global soil carbon  
641 loss attenuated by downward carbon movement, *Glob Chang Biol*, 26, 7242-7254,  
642 10.1111/gcb.15370, 2020.
- 643 Malik, A. A., Puissant, J., Buckeridge, K. M., Goodall, T., Jehmlich, N., Chowdhury,  
644 S., Gweon, H. S., Peyton, J. M., Mason, K. E., van Agtmaal, M., Blaud, A., Clark, I.  
645 M., Whitaker, J., Pywell, R. F., Ostle, N., Gleixner, G., and Griffiths, R. I.: Land use  
646 driven change in soil pH affects microbial carbon cycling processes, *Nature*  
647 *Communications*, 9, 3591, 10.1038/s41467-018-05980-1, 2018.
- 648 Mishra, U., Hugelius, G., Shelef, E., Yang, Y. H., Strauss, J., Lupachev, A., Harden, J.  
649 W., Jastrow, J. D., L., P. C., Riley, W. J., Schuur, E. A. G., Matamala, R., Siewert, M.,  
650 Nave, L. E., Koven, C. D., Fuchs, M., Palmtag, J., Kuhry, P., Treat, C. C., and Zubrzycki,  
651 S.: Spatial heterogeneity and environmental predictors of permafrost region soil organic  
652 carbon stocks, *Science Advances*, 7, 1-12, 10.1126/sciadv.aaz5236, 2021.
- 653 Padarian, J., Minasny, B., McBratney, A., and Smith, P.: Soil carbon sequestration  
654 potential in global croplands, *PeerJ*, 10, e13740, 10.7717/peerj.13740, 2022.
- 655 Patoine, G., Eisenhauer, N., Cesarz, S., Phillips, H. R. P., Xu, X., Zhang, L., and Guerra,  
656 C. A.: Drivers and trends of global soil microbial carbon over two decades, *Nature*  
657 *Communications*, 13, 4195, 10.1038/s41467-022-31833-z, 2022.
- 658 Poffenbarger, H. J., Olk, D. C., Cambardella, C., Kersey, J., Liebman, M., Mallarino,  
659 A., Six, J., and Castellano, M. J.: Whole-profile soil organic matter content,  
660 composition, and stability under cropping systems that differ in belowground inputs,  
661 *Agriculture, Ecosystems & Environment*, 291, 10.1016/j.agee.2019.106810, 2020.
- 662 Qin, S., Yuan, H., Hu, C., Li, X., Wang, Y., Zhang, Y., Dong, W., Clough, T., Luo, J.,  
663 Zhou, S., Wrage-Mönnig, N., Ma, L., and Oenema, O.: Anthropogenic N input  
664 increases global warming potential by awakening the “sleeping” ancient C in deep  
665 critical zones, *Science Advances*, 9, 1-8, doi:10.1126/sciadv.add0041, 2023.
- 666 Reichenbach, M., Fiener, P., Hoyt, A., Trumbore, S., Six, J., and Doetterl, S.: Soil



667 carbon stocks in stable tropical landforms are dominated by geochemical controls and  
668 not by land use, *Global Change Biology*, 29, 2591-2607,  
669 <https://doi.org/10.1111/gcb.16622>, 2023.

670 Rodrigues, L., Hardy, B., Huyghebeart, B., Fohrafellner, J., Fornara, D., Barančíková,  
671 G., Bárcena, T. G., De Boever, M., Di Bene, C., Feizienė, D., Kätterer, T., Laszlo, P.,  
672 O'Sullivan, L., Seitz, D., and Leifeld, J.: Achievable agricultural soil carbon  
673 sequestration across Europe from country-specific estimates, *Global Change Biology*,  
674 27, 6363-6380, <https://doi.org/10.1111/gcb.15897>, 2021.

675 Roland Hiederer. and Köchy, M.: Global Soil Organic Carbon Estimates and the  
676 Harmonized World Soil Database, European Union, 10.2788/13267, 2011.

677 Sanderman, J., Hengl, T., and Fiske, G. J.: Soil carbon debt of 12,000 years of human  
678 land use, *Proceedings of the National Academy of Sciences*, 114, 9575-9580,  
679 doi:10.1073/pnas.1706103114, 2017.

680 Scharlemann, J. P. W., Tanner, E. V. J., Hiederer, R., and Kapos, V.: Global soil carbon:  
681 understanding and managing the largest terrestrial carbon pool, *Carbon Management*,  
682 5, 81-91, 10.4155/cmt.13.77, 2014.

683 Shangguan, W., Dai, Y., Duan, Q., Liu, B., and Yuan, H.: A global soil data set for earth  
684 system modeling, *Journal of Advances in Modeling Earth Systems*, 6, 249-263,  
685 10.1002/2013ms000293, 2014.

686 Soong, J. L., Castanha, C., Hicks Pries, C. E., Ofiti, N., Porras, R. C., Riley, W. J.,  
687 Schmidt, M. W. I., and Torn, M. S.: Five years of whole-soil warming led to loss of  
688 subsoil carbon stocks and increased CO<sub>2</sub> efflux, *Science Advances*, 7,  
689 eabd1343, doi:10.1126/sciadv.abd1343, 2021.

690 Tang, X., Zhao, X., Bai, Y., Tang, Z., Wang, W., Zhao, Y., Wan, H., Xie, Z., Shi, X., Wu,  
691 B., Wang, G., Yan, J., Ma, K., Du, S., Li, S., Han, S., Ma, Y., Hu, H., He, N., Yang, Y.,  
692 Han, W., He, H., Yu, G., Fang, J., and Zhou, G.: Carbon pools in China's terrestrial  
693 ecosystems: New estimates based on an intensive field survey, *Proc Natl Acad Sci U S*  
694 *A*, 115, 4021-4026, 10.1073/pnas.1700291115, 2018.

695 Tao, F., Huang, Y., Hungate, B. A., Manzoni, S., Frey, S. D., Schmidt, M. W. I.,  
696 Reichstein, M., Carvalhais, N., Ciais, P., Jiang, L., Lehmann, J., Wang, Y. P., Houlton,



- 697 B. Z., Ahrens, B., Mishra, U., Hugelius, G., Hocking, T. D., Lu, X., Shi, Z., Viatkin, K.,  
698 Vargas, R., Yigini, Y., Omuto, C., Malik, A. A., Peralta, G., Cuevas-Corona, R., Di  
699 Paolo, L. E., Luotto, I., Liao, C., Liang, Y. S., Saynes, V. S., Huang, X., and Luo, Y.:  
700 Microbial carbon use efficiency promotes global soil carbon storage, *Nature*, 618, 981-  
701 985, 10.1038/s41586-023-06042-3, 2023.
- 702 Wang, C., Qu, L., Yang, L., Liu, D., Morrissey, E., Miao, R., Liu, Z., Wang, Q., Fang,  
703 Y., and Bai, E.: Large-scale importance of microbial carbon use efficiency and  
704 necromass to soil organic carbon, *Glob Chang Biol*, 27, 2039-2048, 10.1111/gcb.15550,  
705 2021a.
- 706 Wang, D., Wu, T., Zhao, L., Mu, C., Li, R., Wei, X., Hu, G., Zou, D., Zhu, X., Chen, J.,  
707 Hao, J., Ni, J., Li, X., Ma, W., Wen, A., Shang, C., La, Y., Ma, X., and Wu, X.: A  
708 1&thinsp;km resolution soil organic carbon dataset for frozen ground in the Third Pole,  
709 *Earth Syst. Sci. Data*, 13, 3453-3465, 10.5194/essd-13-3453-2021, 2021b.
- 710 Wang, J., Wei, X., Jia, X., Huang, M., Liu, Z., Yao, Y., and Shao, M. a.: An empirical  
711 approach to predict regional organic carbon in deep soils, *Science China Earth Sciences*,  
712 66, 583-593, 10.1007/s11430-022-1032-2, 2023.
- 713 Wang, M., Guo, X., Zhang, S., Xiao, L., Mishra, U., Yang, Y., Zhu, B., Wang, G., Mao,  
714 X., Qian, T., Jiang, T., Shi, Z., and Luo, Z.: Global soil profiles indicate depth-  
715 dependent soil carbon losses under a warmer climate, *Nat Commun*, 13, 5514,  
716 10.1038/s41467-022-33278-w, 2022a.
- 717 Wang, Z., Yin, Y., Wang, Y., Tian, X., Ying, H., Zhang, Q., Xue, Y., Oenema, O., Li, S.,  
718 Zhou, F., Du, M., Ma, L., Batchelor, W. D., Zhang, F., and Cui, Z.: Integrating crop  
719 redistribution and improved management towards meeting China's food demand with  
720 lower environmental costs, *Nature Food*, 3, 1031-1039, 10.1038/s43016-022-00646-0,  
721 2022b.
- 722 Wang, H., Yin, Y., Cai, T., Tian, X., Chen, Z., He, K., Wang, Z., Gong, H., Miao, Q.,  
723 Wang, Y., Chu, Y., Zhang, Q., Zhuang, M., & Cui, Z.: Global patterns of soil organic  
724 carbon dynamics in the 20–100 cm soil profile for different ecosystems: A global meta-  
725 analysis [Data set]. Zenodo. <https://doi.org/10.5281/zenodo.10846543>, 2024.
- 726 Wen, S., Chen, J., Yang, Z., Deng, L., Feng, J., Zhang, W., Zeng, X.-M., Huang, Q.,



- 727 Delgado-Baquerizo, M., and Liu, Y.-R.: Climatic seasonality challenges the stability of  
728 microbial-driven deep soil carbon accumulation across China, *Global Change Biology*,  
729 29, 4430-4439, <https://doi.org/10.1111/gcb.16760>, 2023.
- 730 Xia, S., Song, Z., Li, Q., Guo, L., Yu, C., Singh, B. P., Fu, X., Chen, C., Wang, Y., and  
731 Wang, H.: Distribution, sources, and decomposition of soil organic matter along a  
732 salinity gradient in estuarine wetlands characterized by C:N ratio,  $\delta^{13}\text{C}$ - $\delta^{15}\text{N}$ , and  
733 lignin biomarker, *Global Change Biology*, 27, 417-434,  
734 <https://doi.org/10.1111/gcb.15403>, 2021.
- 735 Xu, X., Thornton, P. E., and Post, W. M.: A global analysis of soil microbial biomass  
736 carbon, nitrogen and phosphorus in terrestrial ecosystems, *Global Ecology and*  
737 *Biogeography*, 22, 737-749, [10.1111/geb.12029](https://doi.org/10.1111/geb.12029), 2013.
- 738 Yang, Y., Luo, Y., and Finzi, A. C.: Carbon and nitrogen dynamics during forest stand  
739 development: a global synthesis, *New Phytol*, 190, 977-989, [10.1111/j.1469-](https://doi.org/10.1111/j.1469-8137.2011.03645.x)  
740 [8137.2011.03645.x](https://doi.org/10.1111/j.1469-8137.2011.03645.x), 2011.
- 741 Yulong Yin, Kai He, Zhong Chen, Yangyang Li, Fengling Ren, Zihan Wang, Yingcheng  
742 Wang, Haiqing Gong, Qichao Zhu, Jianbo Shen, Xuejun Liu, and Cui, Z.: Agricultural  
743 Green Development to Coordinate Food Security and Carbon Reduction in the Context  
744 of China's Dual Carbon Goals, *Frontiers of Agricultural Science and Engineering*, 0,  
745 [10.15302/j-fase-2023496](https://doi.org/10.15302/j-fase-2023496), 2023.
- 746 Zhao, G., Bryan, B. A., King, D., Luo, Z., Wang, E., Song, X., and Yu, Q.: Impact of  
747 agricultural management practices on soil organic carbon: simulation of Australian  
748 wheat systems, *Global Change Biology*, 19, 1585-1597,  
749 <https://doi.org/10.1111/gcb.12145>, 2013.
- 750 Zosso, C. U., Ofiti, N. O. E., Torn, M. S., Wiesenberg, G. L. B., and Schmidt, M. W. I.:  
751 Rapid loss of complex polymers and pyrogenic carbon in subsoils under whole-soil  
752 warming, *Nat Geosci*, 16, 344-348, [10.1038/s41561-023-01142-1](https://doi.org/10.1038/s41561-023-01142-1), 2023.